*Articles*

# Crystal Structure of Fragment Double-D from Human Fibrin with Two Different Bound Ligands[†,‡]

Stephen J. Everse,[§] Glen Spraggon,[§] Leela Veerapandian, Marcia Riley, and Russell F. Doolittle*

*Center for Molecular Genetics, University of California, San Diego, La Jolla, California 92093-0634*

*Received February 20, 1998*

ABSTRACT: Factor XIII-cross-linked fragment D (double-D) from human fibrin was crystallized in the presence of two different peptide ligands and the X-ray structure determined at 2.3 Å. The peptide Gly-Pro-Arg-Pro-amide, which is an analogue of the knob exposed by the thrombin-catalyzed removal of fibrinopeptide A, was found to reside in the $\gamma$-chain holes, and the peptide Gly-His-Arg-Pro-amide, which corresponds to the $\beta$-chain knob, was found in the homologous $\beta$-chain holes. The structure shows for the first time that the $\beta$-chain knob does indeed bind to a homologous hole on the $\beta$-chain. The $\gamma$- and $\beta$-chain holes are structurally very similar, and it is remarkable they are able to distinguish between these two peptides that differ by a single amino acid. Additionally, we have found that the $\beta$-chain domain, like its $\gamma$-chain counterpart, binds calcium.

Fibrinogen, the soluble precursor of the fibrin clot, is a covalent dimeric glycoprotein composed of three nonidentical chains ($\alpha_2\beta_2\gamma_2$). The chains are assembled in such a way that all six amino terminals are gathered in a central domain; two terminal globular domains composed of three chains each are tethered to the central domain by three-stranded coiled coils. Limited proteolysis of fibrinogen gives rise to a set of core fragments, the largest of which, fragment D, corresponds to the terminal globules with a residual stump of coiled coil. Limited proteolysis of factor XIII-cross-linked fibrin gives rise to a similar set of fragments, except that the fragments D are themselves cross-linked (*1*, *2*).

The thrombin-catalyzed conversion of fibrinogen to fibrin centers upon the removal of two different pairs of peptides from the amino-terminal regions of the α- and $\beta$-chains. Removal of the fibrinopeptide A from the α-chain leads to the appearance of a new amino-terminal sequence beginning with the sequence Gly-Pro-Arg, whereas removal of the fibrinopeptide B unmasks the sequence Gly-His-Arg. Synthetic peptides based on these beginning sequences are known to bind to fibrinogen and the protease-generated fragment D, but only the Gly-Pro-Arg beginning peptides are effective in inhibiting clot formation (*3*, *4*). In fact, peptides beginning with the sequence Gly-His-Arg actually accelerate the reassociation of fibrin monomers (*3*).

Numerous biochemical experiments over the years have established that the newly exposed Gly-Pro-Arg knobs bind to holes located on the globular carboxyl-terminal region of the $\gamma$-chain. Thus, synthetic Gly-Pro-Arg peptides do not bind to fragment D in which the $\beta$-chain is intact but in which the $\gamma$-chain has been degraded at the carboxyl end (*4*, *5*). Also, photoaffinity labeling experiments with Gly-Pro-Arg derivative peptides led to the exclusive labeling of $Tyr^{\gamma 363}$ (*6*, *7*). Finally, X-ray structures of two different kinds of fragment preparations cocrystallized or soaked with synthetic Gly-Pro-Arg-Pro-amide showed the ligand bound to a hole on the $\gamma$-chain globular domain. In one of these studies (*8*), a 30 kDa recombinant polypeptide corresponding to the $\gamma$-chain carboxyl domain showed the ligand in a well-defined pocket. In the other (*9*), the 170 kDa factor XIII-cross-linked double-D from human fibrin, the GPRPam[1] ligand, was restricted to the hole in the $\gamma$-chain globular domain; the corresponding hole on the homologous domain of the $\beta$-chain was unoccupied. We now report the structure at 2.3 Å of a factor XIII-cross-linked fragment D preparation that was cocrystallized with both GPRPam and GHRPam. The first of these ligands is found in the $\gamma$-chain hole and the second in the $\beta$-chain hole.

Also, during the refinement of the structure, we found that the globular portion of the $\beta$-chain has a bound calcium ion in a site situated much the same as the one in the $\gamma$-chain. This was a wholly unexpected finding, calcium binding in the fragment D portion of fibrinogen long having been thought to be restricted to a single site (*10*) situated on the $\gamma$-chain (*11*−*15*).

[†] This work was supported by Grant HL-26873 from the National Heart, Lung & Blood Institute.

[‡] Atomic coordinates are available from the Brookhaven Protein Data Bank under access code 1FZC.

* To whom correspondence should be addressed. Telephone: (619) 534-4417. Fax: (619) 534-4985. E-mail: rdoolittle@ucsd.edu.

[§] These authors contributed equally to this work.

[1] Abbreviations: GPRPam, Gly-Pro-Arg-Pro-amide; GHRPam, Gly-His-Arg-Pro-amide.

S0006-2960(98)00412-7 CCC: $15.00 © 1998 American Chemical Society
Published on Web 05/21/1998

## MATERIALS AND METHODS

Fibrinogen was purified from plasma obtained from the San Diego Blood Bank. The factor XIII-cross-linked fragment D (double-D) was prepared according to our previously described procedure (*9*). Crystals were obtained by sitting drop, vapor diffusion at room temperature as described previously (*9*, *16*), except preparations were cocrystallized with two different peptides simultaneously. Protein solutions containing 10 mg of fragment double-D per milliliter of 50 mM Tris buffer (pH 7.0), 5 mM $CaCl_2$, 5 mM GPRPam, and 5 mM GHRPam were mixed in equal volumes (5 and 5 $\mu$L) with well solution containing 50 mM Tris (pH 8.0), 10 mM $CaCl_2$, 12% PEG 3350, and 1 mM sodium azide. Crystals appeared only sporadically, but when they did, they were used to streak-seed other solutions that reproducibly yielded good crystals. The drop conditions for streak-seeding differed from those of the initial drops only in that the initial protein concentration was reduced to 5 mg/mL. Synthetic peptides were made by the BOC procedure (*17*) on a Beckman model 990 synthesizer.

All diffraction data were collected at the Cornell High Energy Synchrotron (CHESS) on Beamline A1. A single crystal was flash-frozen in a loop containing 25% PEG 3350 and 25% glycerol. Data were processed with DENZO and ScalePack (*18*). Molecular replacement and subsequent refinement were conducted with routines described in X-PLOR, version 3.843 (*19*), and RefMac as described in the CCP4 suite, version 3.3 (*20*). Modeling was performed on Silicon Graphics computers with the program O (*21*).

Residue numbers used to describe the model are based on human fibrinogen chain numbering (*22*). Figures were generated with a modified version of MOLSCRIPT (*23*) called BOBSCRIPT (*24*) and RASTER3D (*25*, *26*).

## RESULTS

*Molecular Replacement.* Because of the significant change in the unit cell relative to the previously determined structure of the factor XIII-cross-linked double-D (*9*), rigid body refinement could not be performed directly. Accordingly, molecular replacement was undertaken with the model of the 86 kDa fragment D (*9*). Apart from a small change in the central angle (see below), the result is very similar to that for the double-D structure described in our recent report based on a single-ligand preparation, except that the data are of higher resolution and some features in the older model needed modification.

A rotation search was conducted with all data in the resolution range of 8−4 Å. As in the case of double-D with only a single ligand, two solutions were obtained that were approximately 180° apart. The correlation coefficients were 26.3 and 19.2%, respectively, and the corresponding *R*-factors 0.501 and 0.522. The solutions were 11.2$\sigma$ and 8.3$\sigma$ above the mean, respectively. When both solutions were taken together, the correlation coefficient rose to 41.2% and the *R*-factor dropped to 0.472. From this point on, all data between 30 and 2.3 Å were used. SigmaA-weighted electron density maps were constructed (*27*), and both ligands were clearly evident in both $2|F_o - F_c|$ and $|F_o - F_c|$ maps. The model was improved by manual fitting with O. Refinement was accomplished in the early stages with X-PLOR, and in the final stages with RefMac (*28*), during which 432 water molecules were added. In the end, the working *R*-factor was 0.22 and the free *R*-factor (*29*) 0.29 at a resolution of 2.3 Å (Table 1).

Table 1: Data Collection and Refinement Statistics

| | |
|---|---|
| data statistics | |
| space group | $P2_1$ |
| unit cell dimensions | $a = 83.44$ Å, $b = 95.6$ Å, $c = 113.64$ Å, $\beta = 90.19°$ |
| molecules/asymmetric unit | 1 |
| crystals | 1 |
| resolution (Å) | 2.3 |
| observations | 376 448 |
| unique reflections | 81 010 |
| mean redundancy | 4.6 |
| completeness (%) | 94.5 |
| $R_{sym}$ ($I$) (%)[a] | 9.3 |
| refinement statistics | |
| resolution range (Å) | 30.0−2.3 |
| model atoms | 11 152 |
| water molecules | 432 |
| *R*-factor[b] | 0.22 |
| free *R*-factor | 0.29 |
| rms deviations from ideals | |
| bond length (Å) | 0.02 |
| bond angle (deg) | 3.25 |
| average *B*-factor | 36.64 |

[a] $R_{sym} = (\sum|I - \langle I\rangle|)/(\sum|I|)$. [b] Crystallographic *R*-factor $= (\sum||F_o| - |F_c||)/(\sum|F_o|)$ with 95% of the native data for refinement. Free *R*-factor is the *R*-factor based on 5% of the native data withheld from refinement.

Although biochemical analysis indicated that each of the fragments D includes residues $\alpha$111−197, $\beta$134−461, and $\gamma$88−406, amounting to a total of 734 residues in each half of the double-D, the interpretable electron density only includes 683 amino acid residues in each half of the molecule ($\alpha$119−192, $\beta$151−458, and $\gamma$97−397). This is 24 fewer than in our earlier structure, most of the missing residues being at the amino-terminal ends of the coiled coil where the density was more disordered this time. As in our initial report (*9*), the carboxyl-terminal segments of the cross-linked $\gamma$-chains are apparently mobile and could not be discerned in the electron density maps. On the other hand, the electron density in the globular regions of the map was greatly improved, to the point where we could confidently build in an additional residue of the carbohydrate cluster at Asn$^{\beta364}$ (*30*) and adjust the orientation of numerous side chains. In this regard, there are cis peptide bonds at Cys$^{\gamma339}$, as first reported by Pratt et al. (*8*), and the equivalent position in the $\beta$-chain, Cys$^{\beta407}$, as noted in our initial report (*9*).

*General Structure*. The double-D structure with two ligands (GPRPam and GHRPam) (Figure 1A) differs from that with only GPRPam in that its intramolecular angle is about 170° instead of 180° (Figure 1B). To superimpose the structures correctly, it is first necessary to distinguish the two $\gamma$-domains with regard to residues contributing to the asymmetric abutment at the interface. We have arbitrarily designated the $\gamma$-domain whose Arg$^{\gamma275}$ is directed at Ser$^{\gamma300}$ on the opposing domain as A and the $\gamma$-domain whose Arg$^{\gamma275}$ is directed toward an opposing Tyr$^{\gamma280}$ as B. In both structures, the D−D contacts at the polymerization interface are virtually the same, in spite of the flexure. Although it is possible that the difference in angle is a function of flash-freezing, it is noteworthy that the unit cell of the frozen crystal was very similar to that obtained with nonfrozen

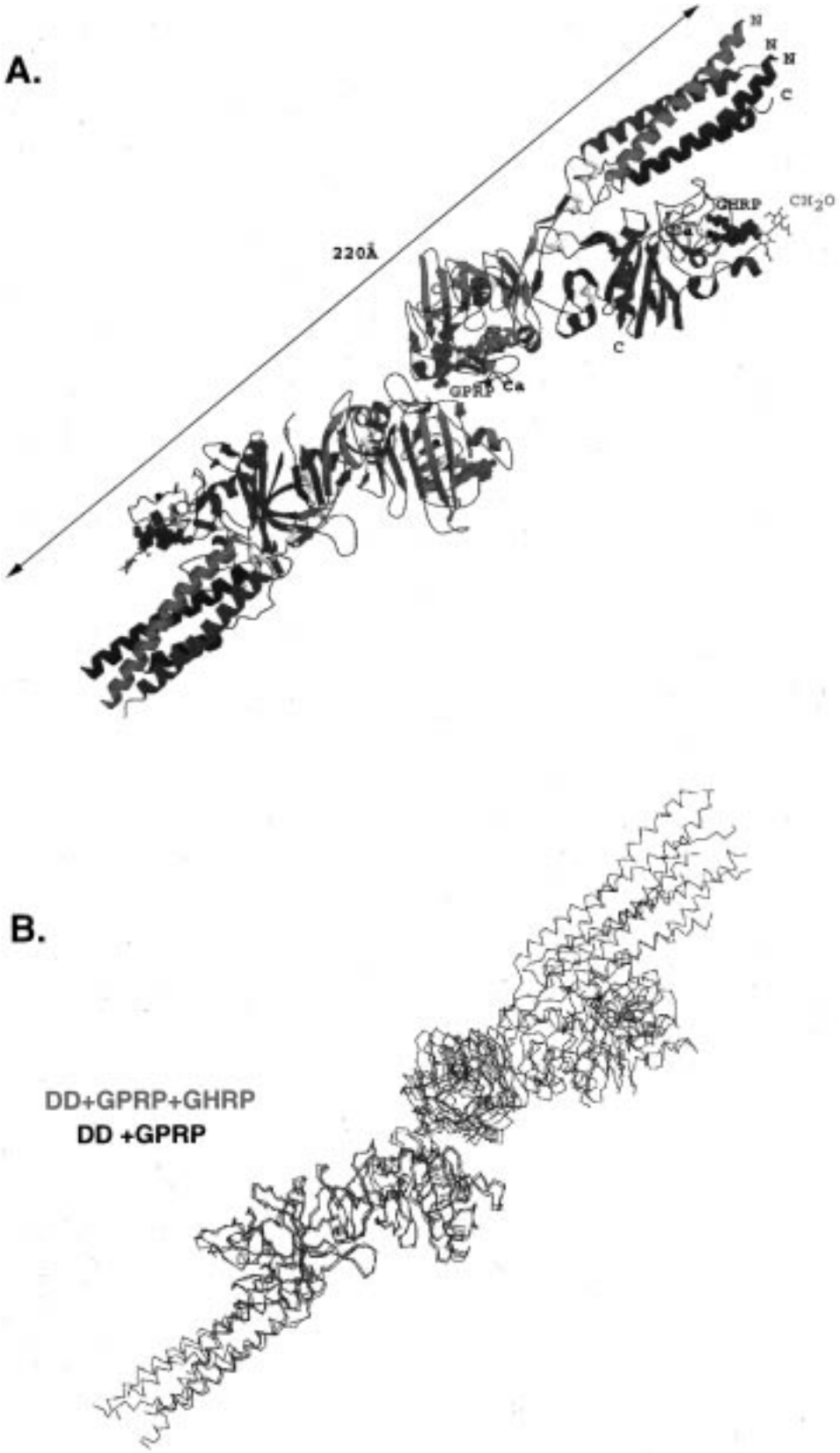


FIGURE 1: (A) α-Carbon backbone structure of double-D from cross-linked human fibrin with two bound ligands. The monomeric units are cross-linked near their carboxyl termini. (B) Superimposed α-carbon backbone structures of double-D with one and two ligands bound (Brookhaven PDB access codes 1FZB and 1FZC).

crystals from the same preparation, and these were significantly different from the unit cell of double-D with only GPRPam bound.

*Peptide Ligands.* $|F_o - F_c|$ omit maps clearly revealed the presence of GPRPam in the $\gamma$-chain holes and GHRPam in the $\beta$-chain holes (Figure 2). The orientation of the

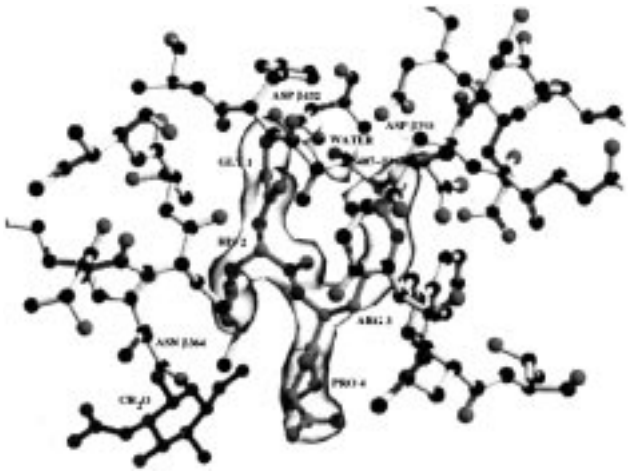

FIGURE 2: Electron density omit map showing the ligand Gly-His-Arg-Pro-amide (GHRPam) bound to the $\beta$-chain binding site in double-D as calculated from $|F_o| - |F_c|$ coefficients and phases from refined model contoured at 2.2$\sigma$. The ligand model was not included in the $F_c$ calculation. Residue numbering based on human fibrinogen.

GHRPam ligand in the pocket is similar to that of the GPRPam (Figure 3). Indeed, the ligand binding sites are almost exactly the same, the one difference being the substitution of a glutamate ($Glu^{\beta 397}$) for a glutamine ($Gln^{\gamma 329}$) (Figure 4). The data also show that both ligands involve a water molecule as a part of the binding constellation (Figure 3). Interestingly, the histidine side chain in GHRPam is oriented so that it is only 3.4 Å from the first GlcNac residue at the base of the carbohydrate cluster (Figure 4B).

*Calcium Binding*. The higher-resolution data revealed a calcium atom bound to the $\beta$-chain at a position equivalent to that of the calcium found in the $\gamma$-chain. The $\beta$-chain calcium only has three coordinating groups: the side chains of $Asp^{\beta 381}$ and $Asp^{\beta 383}$ and the backbone carbonyl of $Trp^{\beta 385}$. The equivalence to the $\gamma$-chain situation is obvious, in which case the equivalent residues are $Asp^{\gamma 318}$, $Asp^{\gamma 320}$, and $Phe^{\gamma 322}$ (Figure 5). The $\gamma$-chain has a fourth coordination site contributed by the backbone carbonyl of $Gly^{\gamma 324}$ that doubtless contributes to its much tighter binding; the fourth coordination site of the $\beta$-chain calcium is apparently provided by an additional water molecule, similar to others

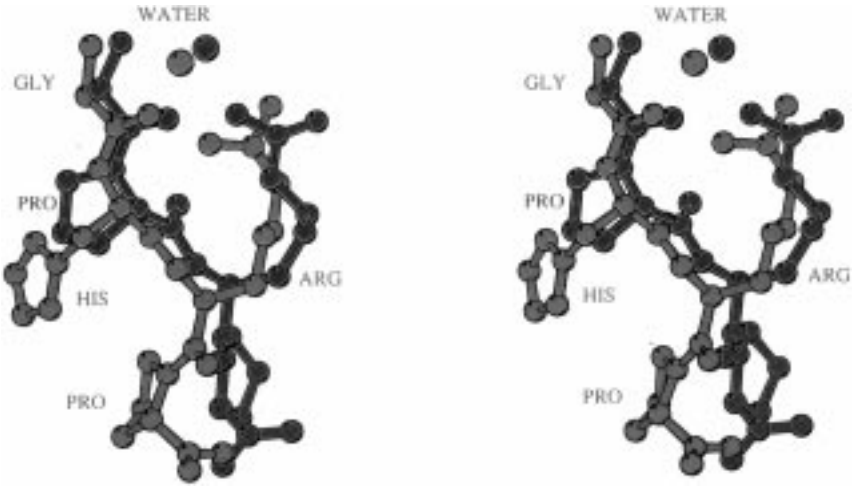


FIGURE 3: Superimposed stereodiagrams of GPRPam and GHRPam as they occur in their respective holes.

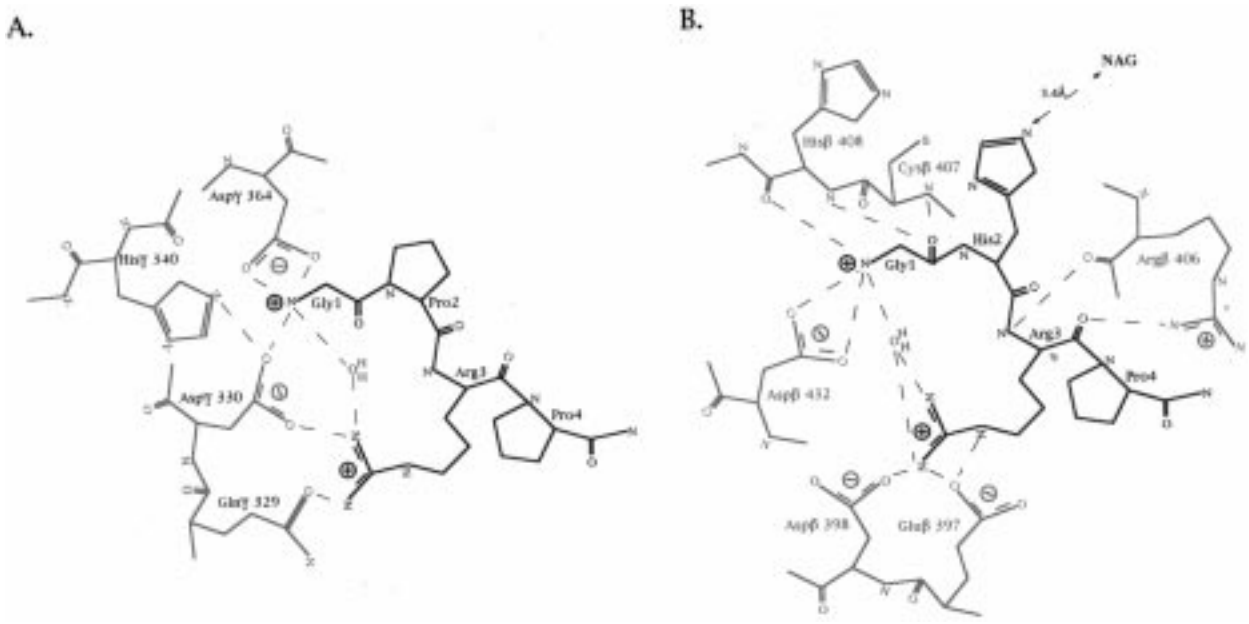


FIGURE 4: Diagrams of attachments for the two ligands GPRPam (A) and GHRPam (B) showing equivalent residues involved in binding.

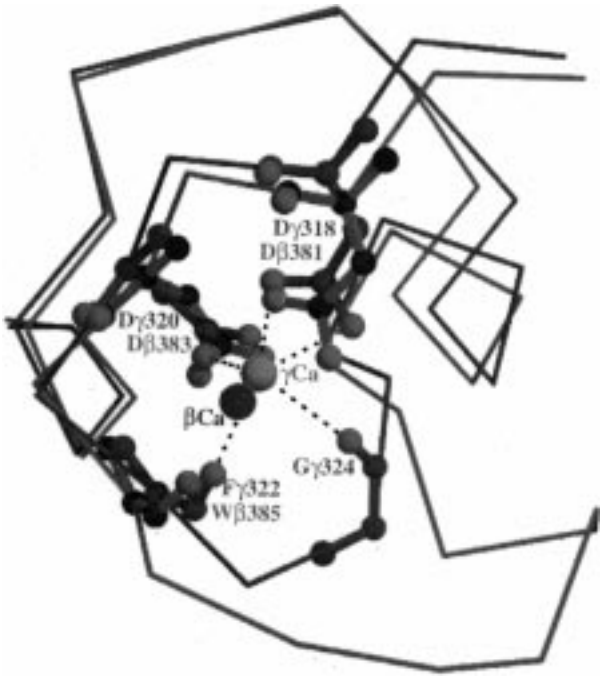


FIGURE 5: Comparison of calcium binding by $\beta$- and $\gamma$-chains showing equivalent residues. The regions shown encompass $\gamma$-chain residues 316−341 and $\beta$-chain residues 379−409.

satisfying the metal's coordination needs.

## DISCUSSION

The role of the fibrinopeptides B and the exposure of $\beta$-chain knobs has been a matter of great debate and conjecture for 40 years. Laurent and Blomback (*31*) suggested that it was the release of the fibrinopeptides A that allowed end-to-end polymerization of the fibrin monmeric units and the release of the fibrinopeptide B that allowed the lateral association of growing protofibrils. Later, when fragmentary sequences of the $\beta$- and $\gamma$-chains made it clear that their carboxyl-terminal domains were homologous (*32*), it seemed logical that they would have similar folds and equivalent binding polymerization sites. In support of this position, Laudano and Doolittle (*3*, *4*) showed that GHRP bound to low-molecular weight fragments D whose $\gamma$-chains had been degraded, even though GPRP did not; subsequently, Medved et al. (*5*) showed that even smaller fragments D were also able to bind GHRP derivatives.

Nonetheless, Gly-His-Arg peptides do not prevent polymerization (*3*, *4*), nor are Gly-His-Arg-substituted supports effective as affinity columns (K. Yamazumi and R. F. Doolittle, unpublished). Similarly, although there are numerous variant human fibrinogens known that have polymerization defects associated with the globular domain of the $\gamma$-chain (*33*, *34*), none has ever been found to be associated with the homologous region of the $\beta$-chain. And although numerous suggestions have been made as to where the hypothetical complementary B sites ought to be (*35*, *36*), the possibilities existed that release of the electronegative fibrinopeptides B merely removed an electrostatic barrier to further association, and that specific knob−hole interactions did not occur. The structure reported here shows that Gly-His-Arg knobs do indeed fit into holes on the $\beta$-chain that are equivalent to those on the $\gamma$-chain. It also shows that previous notions about the general locations of those sites were incorrect.

Thus, release of the fibrinopeptides A exposes two Gly-Pro-Arg knobs that can pin together two other molecules of fibrinogen in an end-to-end fashion. The two holes involved are near the ends of the abutted molecules, and the amino-terminal glycines of the two bound knobs are only 32 Å apart; the α-carbons of the carboxyl-terminal residues of these tetrapeptides (GPRPam) are only 25 Å apart. In contrast, the two $\beta$-chain holes in the double-D structure face opposite directions (Figure 1A), and the glycines of the bound Gly-His-Arg knobs are 146 Å apart; the α-carbons of the carboxyl-terminal residues of these tetrapeptides (GHRPam) are 162 Å apart. Clearly, the orientation of the $\beta$-chain holes is such that a single fibrinogen with centrally situated Gly-His-Arg knobs would have difficulty bridging two other fibrinogen molecules in an end-to-end mode the way the Gly-Pro-Arg knobs do, although, given the 45-residue arm provided by residues $\beta$19−64, it is not altogether impossible. It would seem more reasonable, however, that the spatially preferred knob−hole interaction would be between protofibrils. Past failures of Gly-His-Arg-Pro affinity columns to bind fibrinogen or fragment D may be attributable to steric factors and arms that have not been sufficiently long to reach the $\beta$-chain hole.

*Calcium Binding by the β-Chain*. As first shown by Yee et al. (*37*), the tight binding of calcium by the $\gamma$-chain carboxyl domain is due to four coordinating groups on the protein: the side chains of $Asp^{\gamma 318}$ and $Asp^{\gamma 320}$ and the backbone carbonyls of $Phe^{\gamma 322}$ and $Gly^{\gamma 324}$. In contrast, the binding of the $\beta$-chain calcium involves only three coordinating groups and is obviously weaker than the binding that occurs at the $\gamma$-chain site. The fourth coordination site is absent as a result of a five-residue insertion in this part of the chain (Figure 5) and is likely provided by a water molecule, as are other oxygen atoms needed for filling the coordination shell of the calcium ion.

Initially, the presence of calcium in the $\beta$-chain carboxyl domain surprised us. In retrospect, however, there was reason to have suspected its presence. Thus, although it had been reported that there was a single tight-binding calcium site on fragment D (*10*), Van Ruijuen-Vermeer et al. (*38*) noted that there was also a second site with moderate affinity. Marguerie et al. (*10*) had discounted weaker sites because they were abolished by the presence of 10 mM magnesium ion. It should be noted that the preparations used in our X-ray study were crystallized in the presence of 7.5 mM calcium, a concentration that is somewhat higher than the concentration that exists under physiological conditions (2.5 mM). Nonetheless, straightforward calculations indicate that the site should be occupied under physiological concentrations of calcium and magnesium.

It is also well-known that calcium promotes fibrin formation (*39*), and especially the association of protofibrils in later stages of the process (*40*). There was also reason to think that the calcium effect was correlated with the action of the $\beta$-chain knob. Laudano and Doolittle (*41*) reported that the binding of Gly-His-Arg-Pro to fibrinogen and fragment D is greatly augmented in the presence of calcium, and Furlan et al. (*42*) reported that, in the presence of calcium, Gly-His-Arg peptides inhibited lateral associations. Both of these observations may be attributable to calcium being bound near the $\beta$-chain hole. It should be noted, also, that Van Ruijen-Vermeer et al. (*38*) reported that fragment

double-D actually has a higher affinity for this second site than does fibrinogen. This being the case, calcium may actually modulate later stages of the polymerization process.

Finally, it should be noted that homologues of the $\beta$- and $\gamma$-terminal domains are found in numerous other proteins (*43*), and the two aspartate residues whose side chains are involved in binding calcium are conserved in all known related sequences (upward of 40 reported) except one, tenascin-X, in which the second position is occupied by an asparagine (*44*). It is altogether likely that most fibrinogen-related domains bind calcium at this site.

## REFERENCES


1. Kopec, M., Teisseyre, E., Dudek-Wojciechowska, G., Kloczewiak, M., Pankiewicz, A., and Latallo, Z. S. (1973) *Thromb. Res. 2*, 283−292.
2. Pizzo, S. V., Schwartz, M. L., Hill, R. L., and McKee, P. A. (1973) *J. Biol. Chem. 248*, 4574−4583.
3. Laudano, A. P., and Doolittle, R. F. (1978) *Proc. Natl. Acad. Sci. U.S.A. 75*, 3085−3089.
4. Laudano, A. P., and Doolittle, R. F. (1980) *Biochemistry 19*, 1013−1019.
5. Medved, L. V., Litvinovich, S. V., Ugarova, T. P., Lukinova, N. I., Kalikhevich, V. N., and Ardemasova, Z. A. (1993) *FEBS Lett. 320*, 239−242.
6. Shimizu, A., Nagel, G., and Doolittle, R. F. (1992) *Proc. Natl. Acad. Sci. U.S.A. 89*, 2888−2892.
7. Yamazumi, K., and Doolittle, R. F. (1992) *Proc. Natl. Acad. Sci. U.S.A. 89*, 2893−2896.
8. Pratt, K. P., Cote, H. C. F., Chung, D. W., Stenkamp, R. E., and Davie, E. W. (1997) *Proc. Natl. Acad. Sci. U.S.A. 94*, 7176−7181.
9. Spraggon, G., Everse, S. J., and Doolittle, R. F. (1997) *Nature 389*, 455−462.
10. Marguerie, G., Chagniel, G., and Suscillon, M. (1977) *Biochim. Biophys. Acta 490*, 94−103.
11. Haverkate, F., and Timan, G. (1977) *Thromb. Res. 10*, 803−812.
12. Lawrie, J. S., and Kemp, G. (1979) *Biochim. Biophys. Acta 577*, 415−423.
13. Dang, C. V., Ebert, R. F., and Bell, W. R. (1985) *J. Biol. Chem. 260*, 9713−9717.
14. Varadi, A., and Scheraga, H. A. (1986) *Biochemistry 25*, 519−528.
15. Koopman, J., Haverkate, F., Briet, E., and Lord, S. T. (1991) *J. Biol. Chem. 266*, 13456−13461.
16. Everse, S. J., Pelletier, H., and Doolittle, R. F. (1995) *Protein Sci. 4*, 1013−1016.
17. Merrifield, R. B. (1964) *Biochemistry 3*, 1385−1390.
18. Otwinowski, Z., and Minor, W. (1997) *Methods Enzymol. 276*, 307−326.
19. Brunger, A. T. (1992) *X-PLOR. Version 3.1. A System for X-ray Crystallography and NMR*, Yale University Press, New Haven, CT.
20. Collaborative Computational Project Number 4 (1994) The CCP4 suite: Programs for protein crystallography, version 3.1, *Acta Crystallogr. D50*, 760−763.
21. Jones, T. A., Zou, J.-Y., Cowan, S. W., and Kjeldgaard, M. (1991) *Acta Crystallogr. A47*, 110−119.
22. Doolittle, R. F., Watt, K. W. K., Cottrell, B. A., Strong, D. D., and Riley, M. (1979) *Nature 280*, 464−468.
23. Kraulis, P. J. (1991) *J. Appl. Crystallogr. 24*, 946−950.
24. Esnouf, R. M. (1997) *J. Mol. Graphics 15*, 133−138.
25. Bacon, D. J., and Anderson, W. F. (1988) *J. Mol. Graphics 6*, 219−220.
26. Merritt, E. A., and Murphy, M. E. P. (1994) *Acta Crystallogr. D50*, 869−873.
27. Read, R. J. (1986) *Acta Crystallogr. A42*, 140−149.
28. Murshudov, G. N., Vagin, A. A., and Dodson, E. J. (1997) *Acta Crystallogr. D53*, 240−255.
29. Brunger, A. T. (1992) *Nature 355*, 472−475.
30. Townsend, R. R., Hilliker, E., Li, Y.-T., Laine, R. A., and Bell, W. R. (1982) *J. Biol. Chem. 257*, 9704−9710.
31. Laurent, T. C., and Blomback, B. (1958) *Acta Chem. Scand. 12*, 1875−1977.
32. Takagi, T., and Doolittle, R. F. (1975) *Biochim. Biophys. Acta 386*, 617−622.
33. Ebert, R. F., Ed. (1994) *Index of variant human fibrinogens*, CRC Press, Boca Raton, FL.
34. Everse, S. J., Spraggon, G., and Doolittle, R. F. (1997) *Thromb. Haemostasis* (in press).
35. Olexa, S. A., and Budzynski, A. (1980) *Proc. Natl. Acad. Sci. U.S.A. 77*, 1374−1378.
36. Hasegawa, N., and Sasaki, S. (1990) *Thromb. Res. 57*, 183−195.
37. Yee, V. C., Pratt, K. P., Cote, H. C., LeTrong, I., Chung, D. W., Davie, E. W., Stenkamp, R. E., and Teller, D. C. (1997) *Structure 5*, 125−138.
38. Van Ruijven-Vermeer, I. A. M., Nieuwenhuizen, W., and Nooijen, W. J. (1978) *FEBS Lett. 93*, 177−180.
39. Boyer, M. H., Shainoff, J. R., and Ratnoff, O. D. (1972) *Blood 39*, 382−387.
40. Marx, G. (1987) *Biopolymers 26*, 911−920.
41. Laudano, A. P., and Doolittle, R. F. (1981) *Science 212*, 457−459.
42. Furlan, M., Rupp, C., Beck, E. A., and Svendsen, L. (1982) *Thromb. Haemostasis 47*, 118−121.
43. Doolittle, R. F. (1992) *Protein Sci. 1*, 1563−1577.
44. Morel, Y., Bristow, J., Gitelman, S. E., and Miller, W. L. (1989) *Proc. Natl. Acad. Sci. U.S.A. 86*, 6582−6586.


BI9804129